



## Letter

# Pressure induced by the interaction of water waves with nearly equal frequencies and nearly opposite directions



L. Pellet<sup>a,1</sup>, P. Christodoulides<sup>b</sup>, S. Donne<sup>c</sup>, C.J. Bean<sup>d</sup>, F. Dias<sup>e,\*</sup>

<sup>a</sup> Ecole Centrale Marseille, Marseille, France

<sup>b</sup> Faculty of Engineering and Technology, Cyprus University of Technology, Limassol, Cyprus

<sup>c</sup> School of Earth Sciences, University College Dublin, Belfield Dublin 4, Ireland

<sup>d</sup> School of Cosmic Physics, Dublin Institute for Advanced Studies, Dublin 2, Ireland

<sup>e</sup> School of Mathematics and Statistics, University College Dublin, Belfield Dublin 4, Ireland

## ARTICLE INFO

## Article history:

Received 2 January 2017

Received in revised form 23 March 2017

Accepted 27 March 2017

Available online 25 April 2017

\*This article belongs to the Fluid Mechanics

## Keywords:

Ocean wave–wave interaction

Pressure

Microseisms

## ABSTRACT

We present second-order expressions for the free-surface elevation, velocity potential and pressure resulting from the interaction of surface waves in water of arbitrary depth. When the surface waves have nearly equal frequencies and nearly opposite directions, a second-order pressure can be felt all the way to the sea bottom. There are at least two areas of applications: reflective structures and microseisms. Microseisms generated by water waves in the ocean are small vibrations of the ground resulting from pressure oscillations associated with the coupling of ocean surface gravity waves and the sea floor. They are recorded on land-based seismic stations throughout the world and they are divided into primary and secondary types, as a function of spectral content. Secondary microseisms are generated by the interaction of surface waves with nearly equal frequencies and nearly opposite directions. The efficiency of microseism generation thus depends in part on ocean wave frequency and direction. Based on the second-order expressions for the dynamic pressure, a simple theoretical analysis that quantifies the degree of nearness in amplitude, frequency, and incidence angle, which must be reached to observe the phenomenon, is presented.

© 2017 The Authors. Published by Elsevier Ltd on behalf of The Chinese Society of Theoretical and Applied Mechanics.

This is an open access article under the CC BY-NC-ND license (<http://creativecommons.org/licenses/by-nc-nd/4.0/>).

Microseisms generated by water waves in the ocean occur in the frequency band of 0.05–1.0 Hz. They have been observed from shallow water to deep water [1,2]. Studies have been performed both on the origin of microseisms [3–5] and on their propagation [3,6,7]. Microseisms are produced by the interaction of ocean surface gravity waves and are recorded as “noise” on seismic stations throughout the world. There are two types of microseisms: primary and secondary. Primary microseisms are generated by surface gravity waves incident on a sloping bottom in shallow water and have the same period as the causative waves. Secondary microseisms result from the nonlinear interaction of a pair of linear surface gravity waves of frequencies  $f$  and  $f'$  and wavenumber vectors  $\mathbf{k}$  and  $\mathbf{k}'$ . At second order, in an ocean of depth  $h$ , this interaction leads among other terms to a pressure term with frequency  $f + f'$  and wavenumber vector  $\mathbf{k} + \mathbf{k}'$ . For nearly opposite vectors  $\mathbf{k}$  and  $\mathbf{k}'$  with nearly the same magnitude,  $f + f' \sim 2f$  and  $|\mathbf{k} + \mathbf{k}'|h \ll 1$ . This pressure field thus has a very large phase speed

$2\pi(f + f')/|\mathbf{k} + \mathbf{k}'|$  that can match the horizontal phase speed of acoustic waves in the ocean [8]. Moreover, unlike the other terms in the wave-induced pressure field that decay rapidly with depth, this second-order pressure field is, at a given time, uniform inside the water column except near the free surface. It generates second-order compression waves in the water layer, which in turn play a role in exciting primarily Rayleigh waves at the Earth's surface [9].

As indicated by Arduin and Herbers [4], the slowest noises in the ocean are acoustic-gravity waves that dominate pressure records at depths less than about one-tenth of the acoustic wavelength. These acoustic-gravity waves cannot exist in the absence of ocean surface gravity waves and are thus confined to the region of active wave forcing. Even though the terminology “acoustic-gravity wave” is used, compressibility is not the main driving mechanism and acoustic-gravity waves simply relate to gravity waves that are slightly modified by compressible effects [10]. In this paper, we concentrate on the conditions needed to generate secondary microseisms. Even though compressible effects play a role, we do not take into account these effects. We focus our attention on the pressure fluctuations at double wind-wave or

\* Corresponding author.

E-mail address: [frederic.dias@ucd.ie](mailto:frederic.dias@ucd.ie) (F. Dias).

<sup>1</sup> Now at France Air.

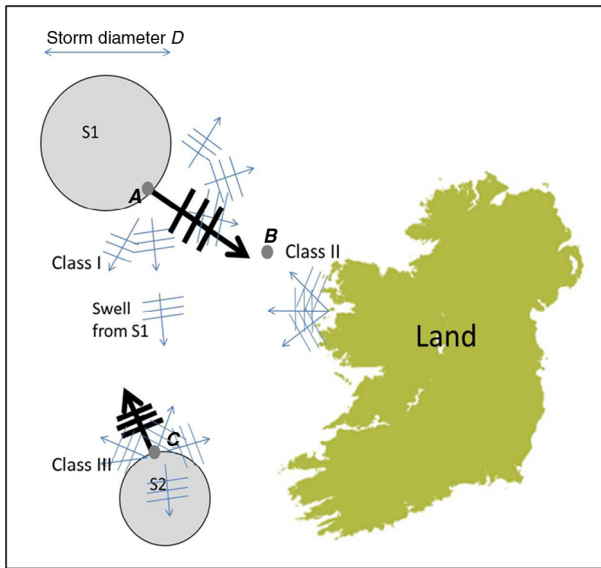


**Fig. 1.** Mechanisms for the generation of secondary microseisms in the ocean wave field.

Source: Modified from Ref. [14].

swell frequencies which can sometimes be observed at the sea floor even in deep water. The attenuation of pressure fluctuations over the water column can be predicted accurately [11,12], and thus pressure measurements in the water column may provide a quantitative verification of numerically modeled directional surface wave properties. In particular, pressure measurements may provide a precise estimate of coastal reflection or wave scattering by currents [13]. Herbers and Guza [11,12] were among the first to provide observations of pressure fluctuations in the water column all the way down to the sea floor that quantitatively support the theoretical mechanism of generation of secondary microseisms. They observed dramatic increases in the spectral levels of seafloor pressure at double wind-wave frequencies after a sudden veering in wind direction resulted in waves propagating obliquely to pre-existing seas. Note that their observations were in intermediate water depth (13 m).

Oceanic secondary microseisms can in principle be generated everywhere. In this paper, we focus on Ireland when it comes to provide precise examples. The main three possibilities to generate secondary microseisms are summarized in Fig. 1. Class I represents a large storm system (S1) which generates wind and waves in many directions, including opposing traveling waves. The Class I mechanism for generating standing waves and secondary microseisms results in a microseism source area near to if not beneath the storm system at point A. Class II describes standing wave generation through coastal reflection of incident traveling waves, generated offshore (e.g. S1). These reflected waves interact with subsequent incident waves to generate standing waves anywhere between the source of the incident waves and the reflecting boundary, point B. Class III refers to the generation of standing waves (point C) through the interaction of local wind sea waves generated at a system (S2) and distant swell from S1. An example of Class I secondary microseisms is given in Ref. [15]. Class II examples are expected to be found on the west coast of Ireland, where cliffs can provide substantial reflection of waves [16]. Examples of Class III secondary microseisms will be given in a companion paper comparing pressure measurements with the analytical expressions of this paper.

Even though pressures induced by water waves with nearly equal frequencies and nearly opposite directions have been known

for a long time in the context of microseisms, they have been largely ignored in the context of reflective structures as insightfully pointed out by Rodriguez et al. [17], see also in Ref. [18]. Indeed second-order pressure fluctuations arise due to the interaction of the first-order incident waves on the structure and the first-order reflected waves. The unattenuated pressure fluctuations at double incident-wave frequency may become the dominant term in deep water.

For all these reasons, it is appropriate to review first the analytical expressions that are already published in the literature to describe the interaction of surface gravity waves [3,4,11–13,19–27]. Some of them, as presented, are lengthy and complicated, while others have some singularities. The main goal of the current study is to give full expressions, not only for the pressure but also for the free surface elevation and the velocity potential. This way we generalize and unify all related expressions in the literature, without any assumption on the water depth. Indeed, as indicated in Fig. 4 of Arduin and Herbers [4], using the deep-water expressions outside of their range can lead to some substantial errors. Besides, misprints occur all too often in the published expressions. The second goal of the paper is to quantify the degree of nearness in amplitude, frequency and incidence angle needed to obtain a significant second-order pressure field that extends all the way to the bottom of the ocean. From the records of coastal seismic stations, one is able to determine wave characteristics (period and height). Therefore, one needs to know the sea states that allow large enough pressure fluctuations at the sea floor capable of generating microseisms. We also need to understand how pressure variations vary in space and time and how they interact with the sea floor. We present the results obtained for the oceanic pressure in different cases, including both two-dimensional (2D) and three-dimensional (3D) regimes. We show the conditions on the various parameters that lead to pressure fluctuations able to generate secondary microseisms.

As stated above, compressible effects play a role in microseisms because of the very long wavelengths involved, but are not dominant for the aspect we consider in this paper, namely the conditions to generate a strong second-order pressure field independent of depth. Therefore, we consider flows in 3D that are irrotational (velocity  $\mathbf{u} = \nabla\phi$ , velocity potential  $\phi(x, y, z; t)$  with  $x$  and  $y$  the horizontal coordinates,  $z$  the vertical coordinate, and  $t$  the time) and periodic in the horizontal directions. The fluid is ideal, incompressible, and homogeneous, with gravity as the only driving force. The flow is bounded below by a flat bottom at  $z = -h$  and above by a free surface at  $z = \eta(x, y; t)$  ( $z = 0$  at rest). Since effects are confined to the region of active wave forcing, the assumption of a flat bottom is not too restrictive.

The governing equations and boundary conditions for the free-surface elevation  $\eta(x, y; t)$  and velocity potential  $\phi(x, y, z; t)$  are

$$\nabla^2\phi = 0, \quad -h < z < \eta, \quad (1)$$

$$\phi_z = 0, \quad z = -h, \quad (2)$$

$$\eta_t + \phi_x\eta_x + \phi_y\eta_y - \phi_z = 0, \quad z = \eta, \quad (3)$$

$$\phi_t + \frac{1}{2}\phi_x^2 + \frac{1}{2}\phi_y^2 + \frac{1}{2}\phi_z^2 + g\eta = 0, \quad z = \eta. \quad (4)$$

The pressure  $p(x, y, z; t)$  is obtained from Bernoulli's equation

$$\begin{aligned} p &= p_a - \rho gz - \rho \left( \phi_t + \frac{1}{2}\phi_x^2 + \frac{1}{2}\phi_y^2 + \frac{1}{2}\phi_z^2 \right) \\ &= p_a - \rho gz + p_d, \end{aligned} \quad (5)$$

where  $p_a - \rho gz$  is the hydrostatic pressure and  $p_d$  the dynamic pressure. From now on, we will set the atmospheric pressure  $p_a$  equal to zero.

$$M_{mn}^{\pm} = \frac{\frac{g^2|\mathbf{k}_m|^2}{\omega_m} + \frac{g^2|\mathbf{k}_n|^2}{\omega_n} - \omega_m^2(\omega_m + 2\omega_n) - \omega_n^2(\omega_n + 2\omega_m) \pm 2g^2\mathbf{k}_m \cdot \mathbf{k}_n\left(\frac{1}{\omega_m} + \frac{1}{\omega_n}\right)}{(\omega_m + \omega_n)^2 - g|\mathbf{k}_m \pm \mathbf{k}_n| \tanh(|\mathbf{k}_m \pm \mathbf{k}_n|h)}, \quad (9)$$

$$N_{mn}^{\pm} = \frac{\frac{g^2|\mathbf{k}_m|^2}{\omega_m} - \frac{g^2|\mathbf{k}_n|^2}{\omega_n} - \omega_m^2(\omega_m - 2\omega_n) + \omega_n^2(\omega_n - 2\omega_m) \pm 2g^2\mathbf{k}_m \cdot \mathbf{k}_n\left(\frac{1}{\omega_m} - \frac{1}{\omega_n}\right)}{\pm[(\omega_m - \omega_n)^2 - g|\mathbf{k}_m \pm \mathbf{k}_n| \tanh(|\mathbf{k}_m \pm \mathbf{k}_n|h)]}. \quad (10)$$

**Box I.**

We assume that the unknown quantities in the system under consideration can be decomposed as

$$\begin{aligned} \eta(x, y, z; t) &= \varepsilon \tilde{\eta}_1 + \varepsilon^2 \tilde{\eta}_2 + O(\varepsilon^3) = \eta_1 + \eta_2 + O(\varepsilon^3), \\ \phi(x, y, z; t) &= \varepsilon \tilde{\phi}_1 + \varepsilon^2 \tilde{\phi}_2 + O(\varepsilon^3) = \phi_1 + \phi_2 + O(\varepsilon^3), \\ p_d(x, y, z; t) &= \varepsilon \tilde{p}_1 + \varepsilon^2 \tilde{p}_2 + O(\varepsilon^3) = p_1 + p_2 + O(\varepsilon^3), \end{aligned} \quad (6)$$

for a small parameter  $\varepsilon$  (typically the sea-surface slope). We choose the origin  $z = 0$  so that  $\eta$  has zero mean value. Applying decomposition Eq. (6) on the governing Eq. (1) (Laplace equation) and on the boundary conditions Eqs. (2)–(4) (bottom boundary condition, kinematic and dynamic conditions on the free surface), we obtain second-order expressions for the free-surface elevation  $\eta$ , the velocity potential  $\phi$ , and the dynamic pressure  $p_d$ . Various regimes are explored in the sequel. Since we are interested in applications to real-world measurements, we work with physical variables that include dimensions.

The superposition of several waves traveling in different directions has been considered by several authors (see Refs. [24,26]). Since the primary focus of the present paper is the quantification of secondary microseisms, we choose for the first-order expression of a train of freely traveling waves (TWs) a form that includes the possibility for each wave of complex amplitude  $A_n$  to have a “sister” wave of complex amplitude  $B_n$  with equal frequency and opposite direction:

$$\eta_1 = \sum_{n=1}^N (A_n e^{i(\mathbf{k}_n \cdot \mathbf{x} - \omega_n t)} - B_n e^{i(\mathbf{k}_n \cdot \mathbf{x} + \omega_n t)} + c.c.), \quad (7)$$

where  $\mathbf{k}_n$  are the wavenumber vectors,  $\omega_n$  the frequencies,  $\mathbf{x} = (x, y)$ ,  $A_n$  and  $B_n$  are the complex amplitudes, and *c.c.* denotes complex conjugate. It is important to emphasize that even though  $\eta_1$  in Eq. (7) was originally written for positive values of  $\omega_n$ , it is equally valid for negative values of  $\omega_n$ . The frequency  $\omega_n$  and the wavenumber vector  $\mathbf{k}_n$  satisfy the dispersion relationship

$$\omega_n^2 = g|\mathbf{k}_n| \tanh(|\mathbf{k}_n|h).$$

There is some redundancy in Eq. (7) since an exact standing wave (SW) can be obtained in several different ways, for example with  $N = 1, A_1 = B_1$  or  $N = 2, A_1 = B_2, \omega_1 = \omega_2, \mathbf{k}_1 = \mathbf{k}_2, A_2 = 0, B_1 = 0$ . Other combinations are possible with negative values of  $\omega$ .

Note that the free-surface elevation Eq. (7) can be used to study a single TW. Simply take  $N = 1$  with  $A_1 \neq 0, B_1 = 0$  or  $B_1 \neq 0, A_1 = 0$ . For example the case of two TWs of different wave numbers and amplitudes traveling in the same direction can be obtained by taking  $B_1 = 0, A_2 = 0$  and replacing  $\omega_2$  by  $-\omega_2$  and  $B_2$  by  $-B_2$ .

The waves in Eq. (7) will interact to give a second-order free-surface elevation given by  $\eta = \eta_1 + \eta_2$ , where

$$\begin{aligned} \eta_2 = \frac{1}{2} \sum_{m=1}^N \sum_{n=1}^N & \left[ \left( M_{mn}^+ \frac{\omega_m + \omega_n}{g} + \frac{\omega_m^2 + \omega_n^2}{g} \right. \right. \\ & \left. \left. + \frac{\omega_m \omega_n}{g} - \frac{g\mathbf{k}_m \cdot \mathbf{k}_n}{\omega_m \omega_n} \right) \right. \end{aligned}$$

$$\begin{aligned} & \times (A_m A_n e^{i((\mathbf{k}_m + \mathbf{k}_n) \cdot \mathbf{x} - (\omega_m + \omega_n)t)} \\ & + B_m B_n e^{i((\mathbf{k}_m + \mathbf{k}_n) \cdot \mathbf{x} + (\omega_m + \omega_n)t)} + c.c.) \\ & - \left( N_{mn}^+ \frac{\omega_m - \omega_n}{g} + \frac{\omega_m^2 + \omega_n^2}{g} - \frac{\omega_m \omega_n}{g} + \frac{g\mathbf{k}_m \cdot \mathbf{k}_n}{\omega_m \omega_n} \right) \\ & \times (A_m B_n e^{i((\mathbf{k}_m + \mathbf{k}_n) \cdot \mathbf{x} - (\omega_m - \omega_n)t)} \\ & + B_m A_n e^{i((\mathbf{k}_m + \mathbf{k}_n) \cdot \mathbf{x} + (\omega_m - \omega_n)t)} + c.c.) \\ & - \left( M_{mn}^- \frac{\omega_m + \omega_n}{g} + \frac{\omega_m^2 + \omega_n^2}{g} + \frac{\omega_m \omega_n}{g} + \frac{g\mathbf{k}_m \cdot \mathbf{k}_n}{\omega_m \omega_n} \right) \\ & \times (A_m \bar{B}_n e^{i((\mathbf{k}_m - \mathbf{k}_n) \cdot \mathbf{x} - (\omega_m + \omega_n)t)} \\ & + B_m \bar{A}_n e^{i((\mathbf{k}_m - \mathbf{k}_n) \cdot \mathbf{x} + (\omega_m + \omega_n)t)} + c.c.) \left. \right] \\ & - \frac{1}{2} \sum_{m=1}^N \sum_{n=1, n \neq m}^N \left( N_{mn}^- \frac{\omega_m - \omega_n}{g} - \frac{\omega_m^2 + \omega_n^2}{g} \right. \\ & \left. + \frac{\omega_m \omega_n}{g} + \frac{g\mathbf{k}_m \cdot \mathbf{k}_n}{\omega_m \omega_n} \right) \\ & \times (A_m \bar{A}_n e^{i((\mathbf{k}_m - \mathbf{k}_n) \cdot \mathbf{x} - (\omega_m - \omega_n)t)} \\ & + B_m \bar{B}_n e^{i((\mathbf{k}_m - \mathbf{k}_n) \cdot \mathbf{x} + (\omega_m - \omega_n)t)} + c.c.), \end{aligned} \quad (8)$$

with  $M_{mn}^{\pm}$  and  $N_{mn}^{\pm}$  given by Eqs. (9) and (10) in Box I.

The kernels  $M_{mn}^{\pm}$  and  $N_{mn}^{\pm}$  have the following properties:

$$N_{mm}^+ = 0, \quad M_{mn}^{\pm} = M_{nm}^{\pm}, \quad N_{mn}^{\pm} = -N_{nm}^{\pm}.$$

The kernel  $N_{mm}^-$  is of the form 0/0. This is not an issue, since all  $N_{mm}^-$  kernels are excluded in the summations above and below.

The expressions for the first-order and second-order velocity potentials are given as

$$\begin{aligned} \phi_1 &= -i \sum_{n=1}^N \frac{g \cosh[|\mathbf{k}_n|(h+z)]}{\omega_n \cosh(|\mathbf{k}_n|h)} (A_n e^{i(\mathbf{k}_n \cdot \mathbf{x} - \omega_n t)} \\ & + B_n e^{i(\mathbf{k}_n \cdot \mathbf{x} + \omega_n t)} - c.c.), \quad (11) \\ \phi_2 &= \frac{i}{2} \sum_{m=1}^N \sum_{n=1}^N \left[ -M_{mn}^+ \frac{\cosh[|\mathbf{k}_m + \mathbf{k}_n|(h+z)]}{\cosh(|\mathbf{k}_m + \mathbf{k}_n|h)} \right. \\ & \times (A_m A_n e^{i((\mathbf{k}_m + \mathbf{k}_n) \cdot \mathbf{x} - (\omega_m + \omega_n)t)} \\ & - B_m B_n e^{i((\mathbf{k}_m + \mathbf{k}_n) \cdot \mathbf{x} + (\omega_m + \omega_n)t)} - c.c.) \\ & + N_{mn}^+ \frac{\cosh[|\mathbf{k}_m + \mathbf{k}_n|(h+z)]}{\cosh(|\mathbf{k}_m + \mathbf{k}_n|h)} \\ & \times (A_m B_n e^{i((\mathbf{k}_m + \mathbf{k}_n) \cdot \mathbf{x} - (\omega_m - \omega_n)t)} \\ & - B_m A_n e^{i((\mathbf{k}_m + \mathbf{k}_n) \cdot \mathbf{x} + (\omega_m - \omega_n)t)} - c.c.) \\ & + M_{mn}^- \frac{\cosh[|\mathbf{k}_m - \mathbf{k}_n|(h+z)]}{\cosh(|\mathbf{k}_m - \mathbf{k}_n|h)} \\ & \times (A_m \bar{B}_n e^{i((\mathbf{k}_m - \mathbf{k}_n) \cdot \mathbf{x} - (\omega_m + \omega_n)t)} \\ & - B_m \bar{A}_n e^{i((\mathbf{k}_m - \mathbf{k}_n) \cdot \mathbf{x} + (\omega_m + \omega_n)t)} - c.c.) \left. \right] \\ & + \frac{i}{2} \sum_{m=1}^N \sum_{n=1, n \neq m}^N N_{mn}^- \frac{\cosh[|\mathbf{k}_m - \mathbf{k}_n|(h+z)]}{\cosh(|\mathbf{k}_m - \mathbf{k}_n|h)} \end{aligned}$$

$$\begin{aligned} & \times (A_m \bar{A}_n e^{i(\mathbf{k}_m - \mathbf{k}_n) \cdot \mathbf{x} - (\omega_m - \omega_n)t} \\ & - B_m \bar{B}_n e^{i(\mathbf{k}_m - \mathbf{k}_n) \cdot \mathbf{x} + (\omega_m - \omega_n)t} - c.c.) \\ & - \sum_{n=1}^N \frac{g^2 |\mathbf{k}_n|^2}{\omega_n^2 \cosh^2(|\mathbf{k}_n| h)} (|A_n|^2 + |B_n|^2) t. \end{aligned} \quad (12)$$

The expressions for the first-order and second-order dynamic pressures are given as

$$\begin{aligned} p_1 &= \rho \sum_{n=1}^N \frac{g \cosh[|\mathbf{k}_n|(h+z)]}{\cosh(|\mathbf{k}_n| h)} (A_n e^{i(\mathbf{k}_n \cdot \mathbf{x} - \omega_n t)} \\ & - B_n e^{i(\mathbf{k}_n \cdot \mathbf{x} + \omega_n t)} + c.c.), \quad (13) \\ p_2 &= \rho \sum_{m=1}^N \sum_{n=1}^N \left\{ \left[ \frac{1}{2} M_{mn}^+ (\omega_m + \omega_n) \right. \right. \\ & \times \left. \frac{\cosh[|\mathbf{k}_m + \mathbf{k}_n|(h+z)]}{\cosh(|\mathbf{k}_m + \mathbf{k}_n| h)} - P_{mn}^- \right] \\ & \times (A_m A_n e^{i(\mathbf{k}_m + \mathbf{k}_n) \cdot \mathbf{x} - (\omega_m + \omega_n)t} \\ & + B_m B_n e^{i(\mathbf{k}_m + \mathbf{k}_n) \cdot \mathbf{x} + (\omega_m + \omega_n)t} + c.c.) \\ & - \left[ \frac{1}{2} N_{mn}^+ (\omega_m - \omega_n) \frac{\cosh[|\mathbf{k}_m + \mathbf{k}_n|(h+z)]}{\cosh(|\mathbf{k}_m + \mathbf{k}_n| h)} + P_{mn}^- \right] \\ & \times (A_m B_n e^{i(\mathbf{k}_m + \mathbf{k}_n) \cdot \mathbf{x} - (\omega_m - \omega_n)t} \\ & + B_m A_n e^{i(\mathbf{k}_m + \mathbf{k}_n) \cdot \mathbf{x} + (\omega_m - \omega_n)t} + c.c.) \\ & - \left. \left[ \frac{1}{2} M_{mn}^- (\omega_m + \omega_n) \frac{\cosh[|\mathbf{k}_m - \mathbf{k}_n|(h+z)]}{\cosh(|\mathbf{k}_m - \mathbf{k}_n| h)} + P_{mn}^+ \right] \right. \\ & \times (A_m \bar{B}_n e^{i(\mathbf{k}_m - \mathbf{k}_n) \cdot \mathbf{x} - (\omega_m + \omega_n)t} \\ & + B_m \bar{A}_n e^{i(\mathbf{k}_m - \mathbf{k}_n) \cdot \mathbf{x} + (\omega_m + \omega_n)t} + c.c.) \left. \right\} \\ & - \rho \sum_{m=1}^N \sum_{n=1, n \neq m}^N \left[ \frac{1}{2} N_{mn}^- (\omega_m - \omega_n) \right. \\ & \times \left. \frac{\cosh[|\mathbf{k}_m - \mathbf{k}_n|(h+z)]}{\cosh(|\mathbf{k}_m - \mathbf{k}_n| h)} + P_{mn}^+ \right] \\ & \times (A_m \bar{A}_n e^{i(\mathbf{k}_m - \mathbf{k}_n) \cdot \mathbf{x} - (\omega_m - \omega_n)t} \\ & + B_m \bar{B}_n e^{i(\mathbf{k}_m - \mathbf{k}_n) \cdot \mathbf{x} + (\omega_m - \omega_n)t} + c.c.) \\ & + \rho \sum_{n=1}^N \frac{g^2 |\mathbf{k}_n|^2 (1 - \cosh[2|\mathbf{k}_n|(h+z)])}{\omega_n^2 \cosh^2(|\mathbf{k}_n| h)} (|A_n|^2 + |B_n|^2), \quad (14) \end{aligned}$$

where

$$\begin{aligned} P_{mn}^\pm &= \frac{g^2 \cosh[|\mathbf{k}_m|(h+z)] \cosh[|\mathbf{k}_n|(h+z)] \mathbf{k}_m \cdot \mathbf{k}_n}{2\omega_m \omega_n \cosh(|\mathbf{k}_m| h) \cosh(|\mathbf{k}_n| h)} \\ & \pm \frac{g^2 \sinh[|\mathbf{k}_m|(h+z)] \sinh[|\mathbf{k}_n|(h+z)] |\mathbf{k}_m| |\mathbf{k}_n|}{2\omega_m \omega_n \cosh(|\mathbf{k}_m| h) \cosh(|\mathbf{k}_n| h)}. \end{aligned} \quad (15)$$

The kernels  $P_{mn}^\pm$  have the following property:

$$P_{mn}^\pm = P_{nm}^\pm.$$

The dynamic pressure at the sea bottom is obtained by replacing  $z$  by  $-h$  in Eqs. (13)–(15).

As indicated by Whitham [28], with the choice of mean value  $\bar{\eta} = 0$ , it is clear from the dynamic condition Eq. (4) on  $z = \eta$  that the mean value  $\bar{\phi}_t$  cannot be zero and  $\phi$  must at least have a term  $t$  in its expansion (the last term in Eq. (12) for  $\phi_2$ ).

All expressions have been checked with Mathematica. The Mathematica files are available upon request. Therefore we are confident that the above expressions are free from typographical errors. As indicated in the introduction, simplifications of these expressions have already been published in the literature by various authors. Some authors give expressions only in deep water, some other authors give expressions for  $\eta$  only. Very few give

expressions for the pressure. Herbers and Guza [11,12] give the expression in integral form. Our original goal was to compare our expressions with all existing ones. The comparison turned out to be too tricky. The recurrent issue seems to be a factor of 2 missing in some expressions. For example, we believe that expression Eq. (3.4) for  $\eta_2$  in Ref. [19] should be divided by a factor of 2. Forristall [22], who reproduced the results of Sharma and Dean [21], writes that his expression Eq. (11) for  $\eta_2$  reduces to Eq. (3.7) of Longuet-Higgins [24], except that the latter equation is missing a factor of 1/2. Dalzell [20] used symbolic computations to derive the expressions for  $\eta_2$  and  $\phi_2$  in finite depth. Dalzell also discussed the limiting cases of progressive waves and standing waves and the issue with the 0/0 limit for  $N_{mn}^-$  when  $n = m$ . Note that we avoid this singular limit in our derivations. Toffoli et al. [27] use again the expressions derived by Sharma and Dean [21]. The first pressure results are those of Longuet-Higgins [3], see also in Ref. [13]. Note that a nice derivation of the pressure together with a clear summary of the various contributions to the pressure, including the second-order pressure pulsation which is spatially uniform and has a frequency twice that of the carrier wave, can be found in Ref. [29]. The most complete results for pressure are those of Ardhuin and Herbers [4], but results for  $\eta_2$  and  $\phi_2$  are not provided. Ardhuin and Herbers compare their results with those of Herbers and Guza [11,12] for the pressure at the sea bottom ( $z = -h$ ). We also checked our expressions against those of Fenton [30] for traveling waves and those of Pierson [26] for interacting long-crested waves on deep water. In both cases, we found agreement.

Now we look at several simplified cases of increasing complexity. More details can be found in Ref. [31]. The first one is the case that was originally studied by Longuet-Higgins [3]. It deals with the superposition of two TWs with opposite wave numbers of the same magnitude and with unequal amplitudes. The second case deals with the superposition of two TWs with opposite wave numbers of different magnitudes and with unequal amplitudes. The third case deals with the superposition of two TWs with different wavenumber vectors and not directly opposing (incidence angle  $\neq 180^\circ$ ). All of these cases can result from various situations encountered in the ocean: coastal reflection, broad storm (single swell event), wind waves interacting with swell.

For two opposite TWs of the same wavenumber  $k$  (and frequency  $\omega$ ) and amplitudes  $A, B$  respectively, Eqs. (7)–(8), (13)–(14) simplify to

$$\eta_1 = A e^{i(kx - \omega t)} - B e^{i(kx + \omega t)} + c.c., \quad (16)$$

$$\begin{aligned} \eta_2 &= k \coth(kh) \left( 1 + \frac{3}{2 \sinh^2(kh)} \right) (A^2 e^{2i(kx - \omega t)} \\ & + B^2 e^{2i(kx + \omega t)} + c.c.) \\ & - k \coth(kh) \left( \frac{1 + \tanh^2(kh)}{2} \right) (AB e^{2ikx} + c.c.), \end{aligned} \quad (17)$$

$$p_1 = \frac{\rho g \cosh[k(h+z)]}{\cosh(kh)} (A e^{i(kx - \omega t)} - B e^{i(kx + \omega t)} + c.c.), \quad (18)$$

$$\begin{aligned} p_2 &= \frac{\rho g k \coth(kh)}{2 \cosh^2(kh)} \left( \frac{3 \cosh[2k(h+z)]}{\sinh^2(kh)} - 1 \right) (A^2 e^{2i(kx - \omega t)} \\ & + B^2 e^{2i(kx + \omega t)} + c.c.) \\ & + \rho g k \coth(kh) \left( 1 + 3 \tanh^2(kh) - \frac{\cosh[2k(h+z)]}{\cosh^2(kh)} \right) \\ & \times (A \bar{B} e^{-2i\omega t} + c.c.) \\ & - \frac{\rho g k \coth(kh)}{\cosh^2(kh)} (AB e^{2ikx} + c.c.) + \frac{\rho g k \coth(kh)}{\cosh^2(kh)} \\ & \times (1 - \cosh[2k(h+z)])(|A|^2 + |B|^2). \end{aligned} \quad (19)$$

In deep water ( $kh \rightarrow \infty$ ), the expressions for  $\eta_2$ ,  $p_1$ , and  $p_2$  reduce to

$$\eta_2 = k(A^2 e^{2i(kx - \omega t)} + B^2 e^{2i(kx + \omega t)} + c.c.) - k(AB e^{2ikx} + c.c.), \quad (20)$$

$$p_1 = \rho g e^{kz} (A e^{i(kx - \omega t)} - B e^{i(kx + \omega t)} + c.c.), \quad (21)$$

$$p_2 = 2\rho\omega^2(2 - e^{2kz})(A\bar{B}e^{-2i\omega t} + c.c.) - 2\rho\omega^2 e^{2kz}(|A|^2 + |B|^2). \quad (22)$$

The second-order dynamic pressure  $p_2$  is independent of  $x$  and its frequency is twice the frequency of the carrier waves. The second term, which decreases exponentially with depth, ensures that the mean water level is zero. The first term, which is felt all the way to the sea bottom, is proportional to the amplitudes of the carrier waves and to the square of their frequency. At the sea bottom ( $z \rightarrow -\infty$ ) (for example, see Ref. [3] or Ref. [29]), it reads

$$p_2 = 8\rho\omega^2 AB \cos(2\omega t),$$

where we have taken for simplicity  $A$  and  $B$  to be real. The amplitude of this second-order pressure oscillation increases when the period of the opposing waves becomes shorter. It is notable that this second-order pressure oscillation is stronger at the sea bottom than at the sea surface Eq. (22).

With this example of two opposite TWs of the same wavenumber, we illustrate the subtleties involved with pressure measurements. The dynamic pressure  $p_d$  is the wave induced pressure, i.e., the excess pressure relative to the hydrostatic pressure  $-\rho g z$  (and the atmospheric pressure, here set equal to zero). At first order,  $p_d = p_1$ . At the free surface  $z = \eta_1$ ,  $p_d = \rho g \eta_1$  since  $p = 0$ , see Eq. (5). Taking  $A$  and  $B$  to be real, one can rewrite the pressure  $p_1$  Eq. (18) as

$$p_1 = \frac{2\rho g \cosh[k(h+z)]}{\cosh(kh)} \sqrt{A^2 + B^2 - 2AB \cos(2kx)} \times \cos(\kappa - \omega t), \quad (23)$$

with

$$\kappa = \tan^{-1} \left[ \frac{(A+B) \sin(kx)}{(A-B) \cos(kx)} \right].$$

The maximum of the pressure  $p_1$  depends on  $x$ . Depending on the values for  $x$ , the following inequality holds for the maximum pressure  $p_1$ :

$$\frac{2\rho g \cosh[k(h+z)]}{\cosh(kh)} |A - B| < \max p_1 < \frac{2\rho g \cosh[k(h+z)]}{\cosh(kh)} |A + B|.$$

At second order,  $p_d = p_1 + p_2$ . Since at the free surface  $z = \eta_1 + \eta_2$ ,  $p_d = \rho g(\eta_1 + \eta_2)$ , see Eq. (5). Therefore it is not easy to distinguish between the various components of the pressure in the vicinity of the free surface. This is why we will only consider the expression of the dynamic pressure  $p_d$  in the lower part of the water column, where  $p_d$  is dominated by the second-order term  $p_2$ , when we investigate the conditions under which a significant second-order dynamic pressure field is present in the subsurface zone.

We now consider two TWs of different wave numbers  $k_1, k_2$  (frequencies  $\omega_1, \omega_2$ ) and amplitudes  $A, B$  respectively, traveling in opposite directions. For deep water waves ( $k_1 h, k_2 h, (k_1 + k_2) h \gg 1$ ),

$$\eta_1 = A e^{i(k_1 x - \omega_1 t)} - B e^{i(k_2 x + \omega_2 t)} + c.c., \quad (24)$$

$$p_1 = \rho g e^{k_1 z} (A e^{i(k_1 x - \omega_1 t)} + c.c.) - \rho g e^{k_2 z} (B e^{i(k_2 x + \omega_2 t)} + c.c.). \quad (25)$$

We provide the value for the dynamic pressure  $p_2$  at the sea bottom ( $z = -h$ ):

$$p_2 = \frac{4\rho\omega_1\omega_2(\omega_1 + \omega_2)^2}{[(\omega_1 + \omega_2)^2 - g(k_1 - k_2) \tanh[(k_1 - k_2)h]] \cosh[(k_1 - k_2)h]} \times (A\bar{B}e^{i[(k_1 - k_2)x - (\omega_1 + \omega_2)t]} + c.c.). \quad (26)$$

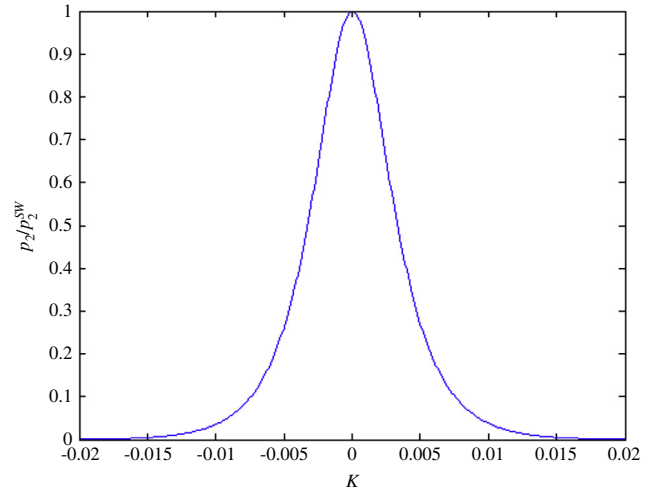


Fig. 2. Dimensionless second-order dynamic pressure  $p_2/p_2^{SW}$  vs.  $K$  in  $m^{-1}$ , for  $k_1 = 0.04 m^{-1}$  and  $h = 400 m$ .

The second-order pressure  $p_2$  is periodic in space ( $k = 2\pi/(k_1 - k_2)$ ) and time ( $T = 2\pi/(\omega_1 + \omega_2)$ ), and proportional to the amplitude of the carrier waves. Let us now investigate the conditions under which  $p_2$  is felt all the way to the sea bottom. We write

$$k_2 = k_1 + K.$$

Then, for a given  $k_1$  and a given  $h$ ,  $p_2$  in Eq. (26) can be thought of as a function of  $K$ :

$$p_2(K) = \frac{4\rho\omega_1^2 \sqrt{1 + K/k_1} (1 + \sqrt{1 + K/k_1})^2}{[(1 + \sqrt{1 + K/k_1})^2 - K \tanh(Kh)/k_1] \cosh(Kh)} \times \left( A\bar{B}e^{i[-Kx - \sqrt{gk_1}(1 + \sqrt{1 + K/k_1})t]} + c.c. \right). \quad (27)$$

When  $K = 0$ , we are back to the case studied. Let (for  $\omega_1 = \omega$ )

$$p_2^{SW} = 8\rho\omega^2 AB.$$

Then, at  $t = 0$  and  $x = 0$ ,

$$p_2(K) = p_2^{SW} \frac{\sqrt{1 + K/k_1} (1 + \sqrt{1 + K/k_1})^2}{[(1 + \sqrt{1 + K/k_1})^2 - K \tanh(Kh)/k_1] \cosh(Kh)}.$$

Assuming that  $h = 400 m$  and  $k_1 = 0.04 m^{-1}$  (corresponding to  $T_1 = 10 s$ ), an illustration for the magnitude of the dimensionless coefficient  $p_2/p_2^{SW}$  is provided in Fig. 2 as function of the wave number difference  $K$ . One can clearly observe that the coefficient decreases rapidly with  $K$ . Already at  $|K| = 0.008 m^{-1}$ , there is a 90% decrease. Although the coefficient is not symmetric in  $K$ , its behavior is nearly identical for both negative and positive values of  $K$ .

While short period standing waves produce second-order pressures of larger amplitude than long period standing waves, they are more sensitive to changes in the characteristics of the opposing interacting waves.

Analogous results with the 2D case can be obtained for the 3D case. Results for two TWs of different wave vectors traveling in opposite direction are presented below at  $z = -h$  ( $p_1 \rightarrow 0$ ). For deep water waves ( $|k_1|h, |k_2|h, |k_1 + k_2|h \gg 1$ ),

$$\eta_1 = A e^{i(k_1 \cdot x - \omega_1 t)} - B e^{i(k_2 \cdot x + \omega_2 t)} + c.c., \quad (28)$$

$$p_1 = \rho g e^{k_1 z} A e^{i(k_1 \cdot x - \omega_1 t)} - \rho g e^{k_2 z} B e^{i(k_2 \cdot x + \omega_2 t)} + c.c. \quad (29)$$

$$p_2(K, \beta) = \frac{2\rho\omega_1^2\sqrt{1+K/|\mathbf{k}_1|}(1+\sqrt{1+K/|\mathbf{k}_1|})^2(1+\cos\beta)}{[(1+\sqrt{1+K/|\mathbf{k}_1|})^2-|\mathbf{k}_1-\mathbf{k}_2|\tanh(|\mathbf{k}_1-\mathbf{k}_2|h)/|\mathbf{k}_1|]\cosh(|\mathbf{k}_1-\mathbf{k}_2|h)} \times (A\bar{B}e^{i[(\mathbf{k}_1-\mathbf{k}_2)\cdot\mathbf{x}-(\omega_1+\omega_2)t]} + c.c.), \quad (31)$$

where

$$|\mathbf{k}_1-\mathbf{k}_2| = \sqrt{2|\mathbf{k}_1|^2-2K|\mathbf{k}_1|-2|\mathbf{k}_1|^2\cos\beta+2K|\mathbf{k}_1|\cos\beta+K^2}.$$

#### Box II.

We provide the value for the dynamic pressure  $p_2$  at the sea bottom ( $z = -h$ ):

$$p_2 = \frac{2\rho[g^2\mathbf{k}_1\cdot\mathbf{k}_2(\frac{1}{\omega_1}+\frac{1}{\omega_2})+\omega_1\omega_2(\omega_1+\omega_2)](\omega_1+\omega_2)}{[(\omega_1+\omega_2)^2-g|\mathbf{k}_1-\mathbf{k}_2|\tanh(|\mathbf{k}_1-\mathbf{k}_2|h)]\cosh(|\mathbf{k}_1-\mathbf{k}_2|h)} \times (A\bar{B}e^{i[(\mathbf{k}_1-\mathbf{k}_2)\cdot\mathbf{x}-(\omega_1+\omega_2)t]} + c.c.). \quad (30)$$

The second-order pressure is periodic in space ( $k = 2\pi/|\mathbf{k}_1 - \mathbf{k}_2|$ ) and time ( $T = 2\pi/(\omega_1 + \omega_2)$ ), and proportional to the carrier waves' amplitudes. The expression is independent of the depth with restrictive conditions on  $|\beta|$  ( $\beta$  is the angle between the two waves) and  $|\delta T|$ . The amplitude of the second order pressure diminishes when  $|\beta|$  and  $|\delta T|$  increase.

To investigate the conditions under which  $p_2$  is felt all the way to the sea bottom, we follow the same procedure as before. We write

$$|\mathbf{k}_2| = |\mathbf{k}_1| + K.$$

Then, for a given  $\mathbf{k}_1$  and a given  $h$ ,  $p_2$  in Eq. (30) can be thought of as a function of  $K$  and  $\beta$  in Eq. (31) of Box II.

As in the previous case, for  $K = 0$ , we can study the magnitude of the dimensionless coefficient  $p_2/p_2^{SW}$  (at  $t = 0$  and  $x = 0$ ) as a function of the wave number difference  $K$  and the angle difference  $\beta$ , as shown in Fig. 3. As before, we assume that  $h = 400$  m and  $|\mathbf{k}_1| = 0.04 \text{ m}^{-1}$  (corresponding to  $T_1 = 10$  s). The coefficient is symmetric in  $\beta$ , and nearly symmetric in  $K$ . Only positive values of  $\beta$  smaller than  $\pi/8$  are shown to better illustrate the fast decay of the second-order dynamic pressure as the angle between the two waves increases.

We have investigated the interaction of water waves of nearly equal frequencies and nearly opposite directions in arbitrary water depth. Second-order expressions were given for the free-surface elevation, velocity potential, and pressure.

For two opposite TWs of the same wave number, the second-order pressure is independent of the depth, periodic in time with twice the frequency of the carrier waves, and proportional to their amplitudes.

For two opposite TWs of different wave numbers, the second-order pressure is dependent of depth in the general case, periodic in time and space, and proportional to their amplitudes.

Extending to the 3D case of TWs of different wave vectors traveling in opposite directions, we still observe the same behavior. The amplitude of the second-order pressure is very sensitive to  $\beta$  (the angle between the waves) and the difference in wave numbers. Small variations in wave numbers cause large variations of the second order pressure amplitude. The maximum in wave number difference to obtain second-order pressure variations that can be detected depends on the value of the period of the carrier wave, and it diminishes when the period diminishes. This could explain why microseisms are very localized in space and time.

The present work can also accommodate the case of irregular swells. However, compressible effects have not been taken into account. This is left for future work.

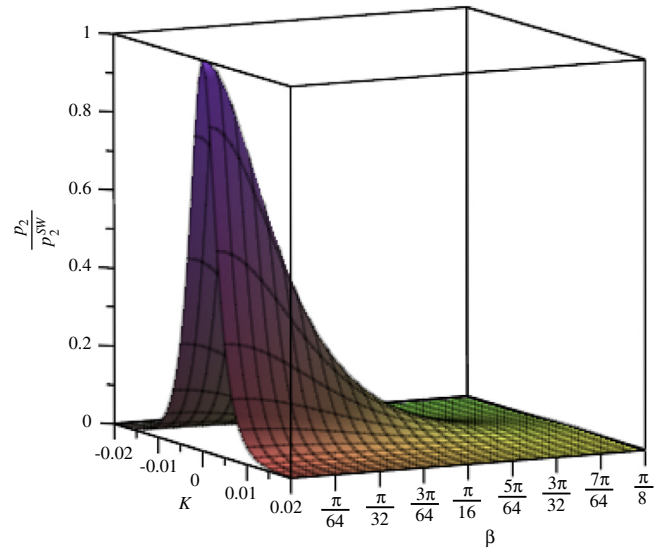


Fig. 3. Dimensionless second-order dynamic pressure  $p_2/p_2^{SW}$  vs.  $K$  and  $\beta$ , for  $k_1 = 0.04 \text{ m}^{-1}$  and  $h = 400$  m.

#### Acknowledgments

This work is partly supported by the Science Foundation Ireland (SFI) under the research project “High-end computational modeling for wave energy systems” (SFI/10/IN.1/12996) in collaboration with Marine Renewable Energy Ireland (MaREI), the SFI Centre for Marine Renewable Energy Research (SFI/12/RC/2302).

#### References

- [1] P.D. Bromirski, Earth vibrations, *Science* 324 (2009) 1026–1027.
- [2] P. Gerstoft, P.D. Bromirski, Weather bomb induced seismic signals, *Science* 353 (2016) 869–870.
- [3] M.S. Longuet-Higgins, A theory of the origin of microseisms, *Philos. Trans. R. Soc. Lond. A* 243 (1950) 1–35.
- [4] F. Ardhuin, T.H.C. Herbers, Noise generation in the solid earth, ocean and atmosphere, from nonlinear interacting surface gravity waves in finite depth, *J. Fluid Mech.* 716 (2013) 316–348.
- [5] F. Ardhuin, E. Stutzmann, M. Schimmel, et al., Ocean wave sources of seismic noise, *J. Geophys. Res.: Oceans* 116 (1978–2012) (2011) C09004.
- [6] K. Hasselmann, Ocean wave sources of seismic noise, *Rev. Geophys.* 1 (1963) 177–210.
- [7] Y. Ying, C.J. Bean, P.D. Bromirski, Propagation of microseisms from the deep ocean to land, *Geophys. Res. Lett.* 41 (2014) 6374–6379. <http://dx.doi.org/10.1002/2014GL060979>.
- [8] F. Ardhuin, T. Lavanant, M. Obrebski, et al., A numerical model for ocean ultra-low frequency noise: Wave generated acoustic-gravity and Rayleigh modes, *J. Acoust. Soc. Am.* 134 (2013) 3242–3259.
- [9] M.S. Longuet-Higgins, Can sea waves cause microseisms? in: *Proc. Symposium on Microseisms*, Earriman, N.Y., U.S.A., vol. 306, 1953, pp. 74–86.

- [10] E. Renzi, F. Dias, Hydro-acoustic precursors of gravity waves generated by surface pressure disturbances localised in space and time, *J. Fluid Mech.* 754 (2014) 250–262.
- [11] T.H.C. Herbers, R.T. Guza, Wind-wave nonlinearity observed at sea floor. Part I: Forced-wave energy, *J. Phys. Oceanogr.* 21 (1991) 1740–1761.
- [12] T.H.C. Herbers, R.T. Guza, Nonlinear wave interactions and high-frequency seafloor pressure, *J. Geophys. Res.* 99 (1994) 10035–10048.
- [13] R.I.B. Cooper, M.S. Longuet-Higgins, An experimental study of the pressure variations in standing water waves, *Proc. R. Soc. Lond. Ser. A Math. Phys. Eng. Sci.* 206 (1951) 426–435.
- [14] F. Ardhuin, A. Balanche, E. Schimmel, et al., From seismic noise to ocean wave parameters: General methods and validation, *J. Geophys. Res.* 117 (2012) C05002.
- [15] M.J. Obrebski, F. Ardhuin, E. Stutzmann, et al., How moderate sea states can generate loud seismic noise in the deep ocean, *Geophys. Res. Lett.* 39 (2012) L11601.
- [16] R. Tiron, S. Gallagher, F. Dias, The influence of coastal morphology on the wave climate and wave energy resource of the west Irish coast, in: *Proceedings of EWTEC 2013, Denmark, 2013*.
- [17] M. Rodriguez, J. Spinneken, C. Swan, Nonlinear loading of a two-dimensional heaving box, *J. Fluids Struct.* 60 (2016) 80–96.
- [18] N. Jarry, Etudes expérimentales et numériques de la propagation des vagues au-dessus de bathymétries complexes en milieu côtier (Ph.D. thesis), Université du Sud Toulon Var, 2009.
- [19] T.A.A. Adcock, P.H. Taylor, Estimating ocean wave directional spreading from an Eulerian surface elevation time history, *Proc. R. Soc. Lond. Ser. A Math. Phys. Eng. Sci.* 465 (2009) 3361–3381.
- [20] J.F. Dalzell, A note on finite depth second-order wave-wave interaction, *Appl. Ocean Res.* 21 (1999) 105–111.
- [21] R.G. Dean, J.N. Sharma, Simulation of wave systems due to nonlinear directional spectra, in: *Int. Symp. on Hydrodynamics in Coastal Engineering, Trondheim, 1981*, pp. 1211–1222.
- [22] G.Z. Forristall, Wave crest distributions: Observations and second-order theory, *J. Phys. Oceanogr.* 30 (2000) 1931–1943.
- [23] M.S. Longuet-Higgins, Resonant interaction between two trains of gravity waves, *J. Fluid Mech.* 12 (1962) 321–332.
- [24] M.S. Longuet-Higgins, The effect of non-linearities on statistical distributions in the theory of sea waves, *J. Fluid Mech.* 17 (1963) 459–480.
- [25] P.A. Madsen, D.R. Fuhrman, Third-order theory for multi-directional irregular waves, *J. Fluid Mech.* 698 (2012) 304–334.
- [26] W.J. Pierson, Oscillatory third-order perturbation solutions for sums of interacting long-crested Stokes waves on deep water, *J. Ship Res.* 37 (1993) 354–383.
- [27] A. Toffoli, M. Onorato, A.V. Babanin, et al., Second-order theory and setup in surface gravity waves: A comparison with experimental data, *J. Phys. Oceanogr.* 37 (2007) 2726–2739.
- [28] G.B. Whitham, *Linear and Nonlinear Waves*, John Wiley & Sons, 1974.
- [29] O.M. Phillips, *The Dynamics of the Upper Ocean*, Cambridge University Press, 1977.
- [30] J.D. Fenton, Nonlinear wave theories, in: *The Sea*, in: *Ocean Engineering Science*, vol. 9, Wiley, New York, 1990.
- [31] L. Pellet, *Assessing Ocean Wave Energy Potential from Land Based Observations*, Ecole Centrale Marseille, 2013.